# Solution processable donor–acceptor oligothiophenes for bulk-heterojunction solar cells†

**Weifeng Zhang,[a] Shing Chi Tse,[b] Jianping Lu,[b] Ye Tao*[b] and Man Shing Wong*[a]**

***Received 14th December 2009, Accepted 24th December 2009***
***First published as an Advance Article on the web 2nd February 2010***
**DOI: 10.1039/b926203b**



Novel p-type and low bandgap penta- and hexa-thiophenes asymmetrically endcapped with solubilizing triarylamine or triarylamino-substituted carbazole dendron and dicyanovinyl groups, namely, **PhNOF-OT(*n*)-DCN** and **$G_2$-OT(*n*)-DCN**, respectively where $n = 5$–6 for solution-processable photovoltaic applications have been synthesized and investigated. With the incorporation of a solubilizing electron-donating group, the highly extended oligothiophenes are highly soluble in common organic solvents and solution-processable. Upon extending the oligothiophene backbone, there is a strong increase in the absorption around 420 nm in addition to the intramolecular charge-transfer absorption (520 nm) which results in a strong spectral broadening. The optical band-gap of these donor–acceptor oligothiophene thin-films greatly reduces to 1.85 eV. The solution-processed bulk heterojunction PV cells fabricated from these materials blended with PCBM as an acceptor showed a *PCE* up to 1.72% with $V_{oc} = 0.79$ V in an as-fabricated device. Our findings also suggest that highly extended donor–acceptor oligomers can be useful for a p-type, low-bandgap semiconductor for solution-processable bulk heterojunction PV cells.

## Introduction

Organic photovoltaic (PV) cells, which directly convert sunlight into electricity, have drawn considerable attention from both academia and industry because of their promise as low-cost, lightweight, renewable energy sources.[1] Heterojunction PV cells based on solution-processable conjugated p-type semiconducting materials blended with a soluble fullerene derivative, [6,6]-phenyl $C_{61}$-butyric acid methyl ester (PCBM) offer advantages of facile and large-area fabrication on flexible substrates by various printing or coating techniques or a roll-to-roll process[2] affording high power conversion efficiencies (*PCE*) of greater than 6% recently.[3] However, the structural characteristics including molecular weight, polydispersity, and regioregularity as well as the purity of the polymer greatly affect its functional properties, the performance and the stability[4] of the resulting devices. In addition to polymers, π-conjugated small molecules have been found attractive as alternative solution-processable p-type donor materials because of monodispersity, ease of obtaining in high purity and reproducible properties. Nevertheless, the use of solution-processable small molecules for PV applications has drawn considerable attention.[5] Recently, a *PCE* of 1.17% was obtained from a solution-processed BHJ solar cell using an anthracene-core donor and $C_{61}$-PCBM acceptor.[6] In addition, a small molecule PV cell based on the blend of a benzothiadiazole derivative and $C_{61}$-PCBM showed a *PCE* of 2.4% in the annealed device.[7] A high *PCE* of 3.0% has very recently been demonstrated based on an oligothiophene-diketopyrrolepyrrole and $C_{71}$-PCBM blend.[8] To achieve a high efficiency heterojunction PV cell, it is fundamentally important to develop new p-type π-conjugated small molecules with a narrow energy bandgap to harvest more solar radiation and a high charge carrier mobility to transport the photogenerated charges to the electrodes.[9]

Oligothiophenes endcapped with triarylamino and dicyanovinyl or tricyanovinyl groups, which exhibit low optical gap absorption and possess a large enough LUMO level offset with the PCBM acceptors for efficient exciton dissociation, have been shown to be useful for a high performance bilayer heterojunction photovoltaic cell.[10] Nevertheless, these molecules were not suitable for solution-processable bulk heterojunction PV cells. For application in solution-processable bulk heterojunction PV cells, the materials need to have good solubility and thin-film forming properties.[8] To promote the solution-processable properties of small molecule donors, we have developed a novel series of highly extended oligothiophenes asymmetrically endcapped with a solubilizing triarylamine or triarylamino-substituted dendron and a dicyanovinyl group as a p-type, low-optical-gap semiconductor for solution-processable bulk heterojunction PV cells. The use of a highly extended π-conjugated system not only lowers the optical bandgap and promotes strong π–π stacking of conjugated backbones but also increases the absorption and broadens the absorption spectrum as compared to the lower homologues.

We report herein the synthesis and molecular properties of novel p-type and low bandgap penta- and hexa-thiophenes asymmetrically endcapped with solubilizing triarylamine or triarylamino-substituted carbazole dendron and dicyanovinyl

[a]*Department of Chemistry and Centre for Advanced Luminescence Materials, Hong Kong Baptist University, Kowloon Tong, Hong Kong, SAR, China. E-mail: mswong@hkbu.edu.hk*
[b]*Institute for Microstructural Sciences (IMS), National Research Council of Canada (NRC), 1200 Montreal Road, Ottawa, ON K1A 0R6, Canada. E-mail: Ye.Tao@nrc-cnrc.gc.ca*

† Electronic supplementary information (ESI) available: Physical characterization and spectra of new compounds. See DOI: 10.1039/b926203b

 

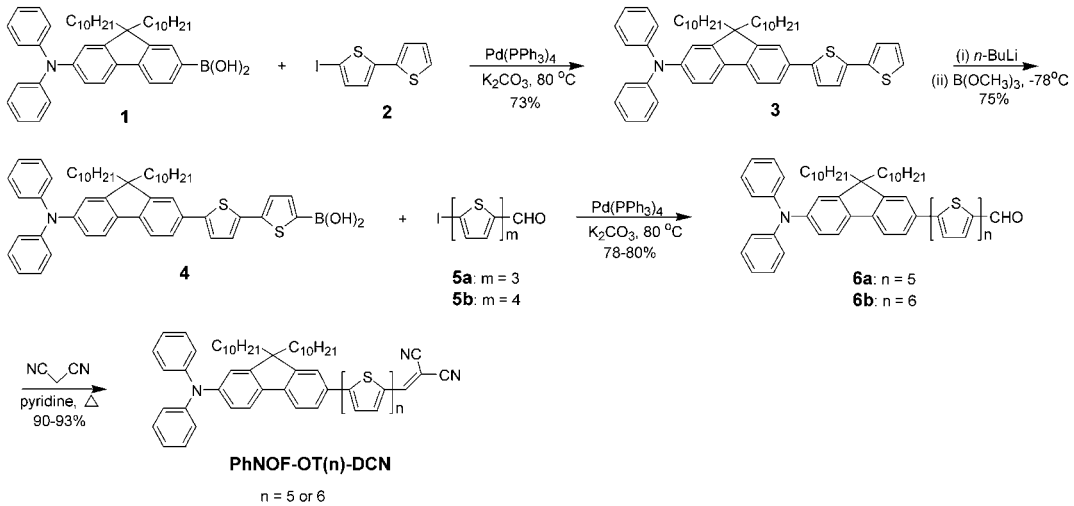


**Scheme 1** Synthesis of triarylamine dicyanovinyl asymmetrically disubstituted oligothiophenes, **PhNOF-OT(*n*)-DCN**, $n = 5$ or 6.

groups, namely, **PhNOF-OT(*n*)-DCN** and **$G_2$-OT(*n*)-DCN**, respectively where $n = 5$–6 for solution-processable photovoltaic applications. With the incorporation of a solubilizing electron-donating group, the highly extended oligothiophenes are highly soluble in common organic solvents and solution-processable. The optical band-gap of these donor–acceptor oligothiophene thin-films greatly reduces to 1.85 eV. The solution-processed bulk heterojunction PV cells fabricated from these materials blended with PCBM as acceptors showed a *PCE* up to 1.72% with $V_{oc} = 0.79$ V in an as-fabricated device. Our findings also suggest that highly extended donor–acceptor oligomers can be used as a p-type, low-bandgap semiconductor for solution-processable bulk heterojunction PV cells.

## Results and discussion

The synthesis of novel triarylamine and dicyanovinyl asymmetrically disubstituted oligothiophenes is outlined in Scheme 1. By adapting the convergent approach used previously,[10] the palladium-catalyzed Suzuki cross-coupling of 7-diphenylamino-9,9-di-*n*-decylfluorenyl-2-boronic acid **1** and iodobithiophene **2** in the presence of $Pd(PPh_3)_4$ as a catalyst afforded the desired

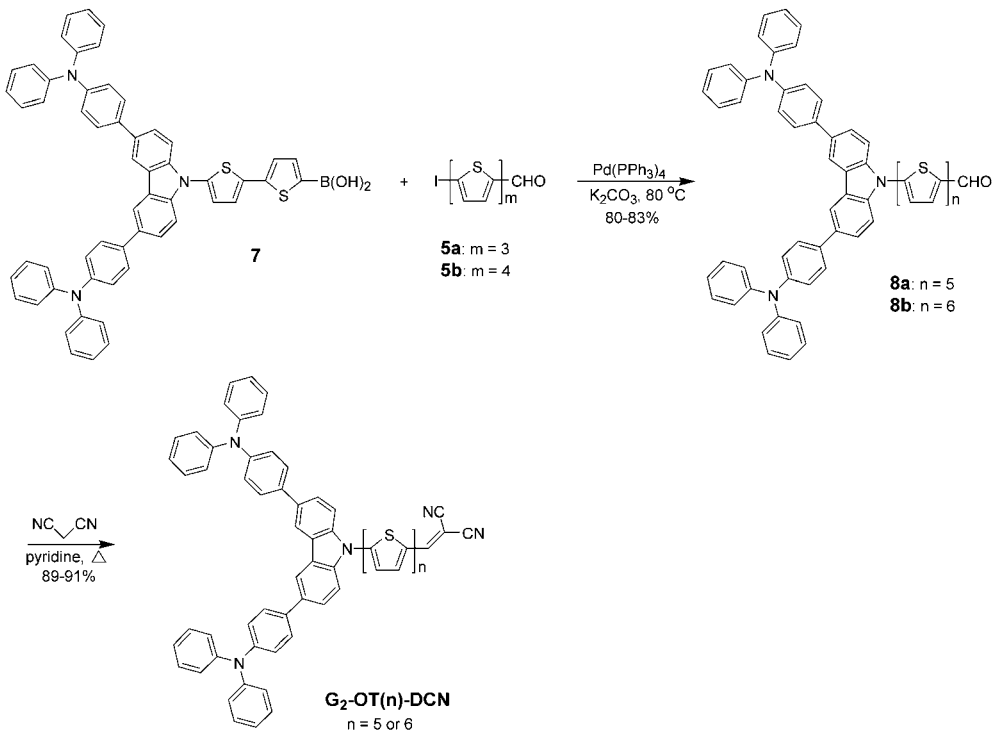


**Scheme 2** Synthesis of triarylamino-substituted carbazole dendron and dicyanovinyl asymmetrically disubstituted oligothiophenes **$G_2$-OT(*n*)-DCN**, $n = 5$ or 6.

diphenylaminofluorenyl-substituted bithiophene **3** in 73% yield. Lithiation of **3** at −78 °C followed by quenching with trimethylborate and subsequently acid hydrolysis afforded the corresponding boronic acid **4** in a good yield. The palladium catalyzed Suzuki cross-coupling of 7-diphenylamino-9,9-di-*n*-decylfluorenyl-5′-bithiophene-5-boronic acid **4** with iodoter- or iodoquater-thiophenecarboxaldehyde **5a** or **5b** afforded the desired diphenylaminofluorenyl-substituted penta- and hexa-thiophenecarboxaldehydes, **6a** and **6b**, respectively in good yields (78–80%). Condensation of these aldehydes **6a** or **6b**, with malononitrile in the presence of pyridine in refluxing chloroform afforded the desired donor–acceptor oligothiophenes **PhNOF-OT(*n*)-DCN**, $n = 5$ or 6 in excellent yields. Furthermore, the synthesis of novel triarylamine-substituted carbazole dendron and dicyanovinyl asymmetrically disubstituted oligothiophenes is outlined in Scheme 2. 5-{3,6-Bis[4-(diphenylamino)-1-phenyl]carbazol-9-yl}-2-bithiophene-boronic acid, **7** was prepared according to the previously published protocol.[5f] The palladium catalyzed Suzuki cross-coupling of boronic acid **7** with iodoter- or iodoquater-thiophenecarboxaldehyde **5a** or **5b** afforded the desired triarylamine-substituted dendritic penta- and hexa-thiophenecarboxaldehydes, **8a** and **8b**, respectively in good yields (80–83%). Similarly, subsequent condensation of **8a** or **8b** with malononitrile afforded the triarylamine-substituted carbazole dendron and dicyanovinyl asymmetrically disubstituted oligothiophenes **G$_2$-OT(*n*)-DCN**, $n = 5$ or 6 in 89–91% yields. All the newly synthesized donor–acceptor oligothiophenes were fully characterized with $^1$H NMR, $^{13}$C NMR, MALDI-TOF MS, and elemental analysis and found to be in good agreement with their structures.

The thermal behaviour and stability of these donor–acceptor oligothiophenes were investigated by DSC and TGA analyses, respectively. The results are summarized in Table 1. The triarylamine-substituted oligothiophenes, **PhNOF-OT(*n*)-DCN** exhibit no apparent glass transition except a melting transition ($T_m$) in the range of 199–217 °C; on the other hand, the dendron-substituted oligothiophenes, **G$_2$-OT(*n*)-DCN** show distinct and high glass transition temperatures with $T_g > 144$ °C suggesting that these dendrimers can form morphologically stable amorphous thin films. All the oligothiophenes exhibit an excellent thermal stability with $T_d$ in the range of 440–515 °C. (Fig. 1)

The absorption spectra of these donor–acceptor oligothiophenes measured in chloroform and DMSO as shown in Fig. 2 are composed of three broad and structureless absorption bands, a weak to strong absorption in the range of 310–330 nm corresponding to the n → π* transition of the arylamine moiety of the triarylamine-based donating group, a moderate to strong absorption around 410–420 nm corresponding to the transition of the extended oligothiophene core, and the long wavelength absorption ($\lambda_{max}^{abs}$) around 520 nm corresponding to the intramolecular charge-transfer (ICT) transition. The $\lambda_{max}^{abs}$ remains fairly constant for **PhNOF-OT(*n*)-DCN**s and shifts slightly to a longer wavelength for **G$_2$-OT(*n*)-DCN**s when the oligothienyl core extends from five to six indicating the approach of the effective conjugation length for the series. It is worth mentioning that in addition to ICT, the enhancement of the absorption around 420 nm upon extending the oligothiophene backbone gives rise to a strong spectral broadening. These oligomers also exhibit an inverted solvatochromic effect upon an increase in

**Table 1** Summaries of physical measurement of **PhNOF-OT(*n*)-DCN** and **G$_2$-OT(*n*)-DCN**

| | $\lambda_{max}^{em}$ [a]/nm ($10^4$ M$^{-1}$ cm$^{-1}$) | Optical gap[a,b]/eV | $E^{oxd}_{1/2}$ or $E^{oxd\ c}_{p}$/V | $E^{red\ c}_{p}$/V | HOMO[d]/eV | LUMO[d]/eV | Energy gap[e]/eV | $T_f$[f]/°C | $T_{dec}$[i]/°C |
|---|---|---|---|---|---|---|---|---|---|
| **PhNOF-OT(5)-DCN** | 526 (5.73) | 1.88 | 0.30, 0.42, 0.86 | −1.44, −2.01 | −5.10 | −3.36 | 1.74 | 199[g] | 440 |
| **PhNOF-OT(6)-DCN** | 524 (6.55) | 1.85 | 0.30, 0.39, 0.73 | −1.41, −1.98 | −5.10 | −3.39 | 1.71 | 217[g] | 460 |
| **G$_2$-OT(5)-DCN** | 518 (5.17) | 1.91 | 0.36, 0.49, 0.79 | −1.55, −2.04 | −5.16 | −3.25 | 1.91 | 144[h] | 514 |
| **G$_2$-OT(6)-DCN** | 522 (5.42) | 1.88 | 0.35, 0.48, 0.73 | −1.55, −2.03 | −5.15 | −3.25 | 1.90 | 148[h] | 515 |

[a] Measured in $CHCl_3$. [b] Estimated from the absorption edge of thin-film. [c] Determined by the CV method using platinum disc electrode as a working electrode, platinum wire as a counter electrode and SCE as a reference electrode with an agar salt bridge connecting to the oligomer solution and ferrocene was used as an external standard, $E_{1/2}$ ($Fc/Fc^+$) = 0.49 V *vs.* SCE. [d] Calculated from the first oxidation or reduction potential with ferrocene (4.8 eV *vs.* vacuum). [e] Energy gap = HOMO–LUMO. [f] Determined by differential scanning calorimeter from re-melt after cooling with a heating rate of 10 °C min$^{-1}$ under $N_2$. [g] Melting point. [h] Glass transition. [i] Determined by thermal gravimetric analyzer with a heating rate of 10 °C min$^{-1}$ under $N_2$.

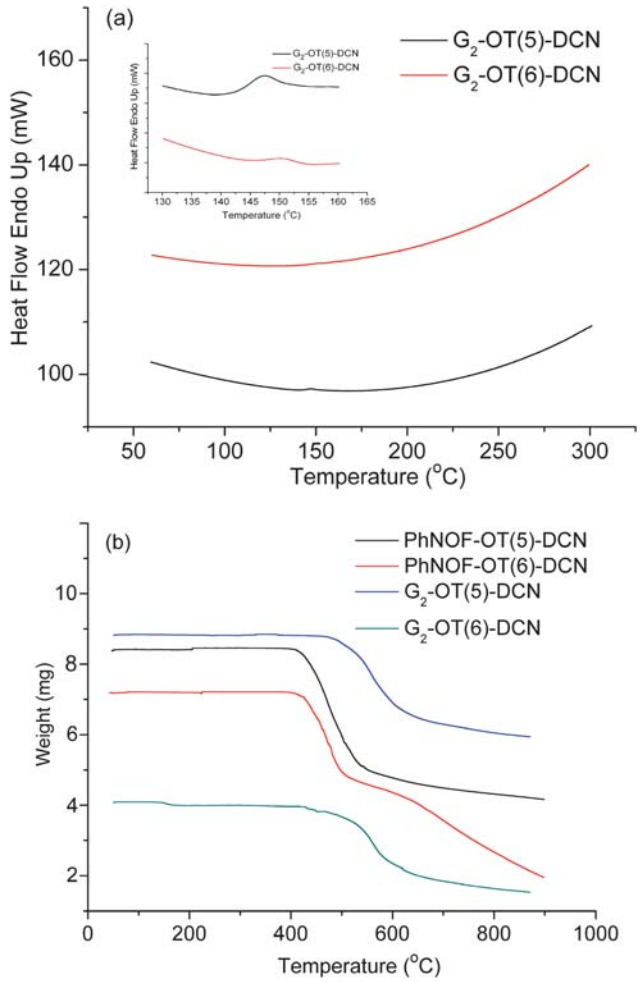


**Fig. 1** (a) DSC traces of **$G_2$-OT(*n*)-DCN**. (b) TGA traces of **PhNOF-OT(*n*)-DCN** and **$G_2$-OT(*n*)-DCN**.

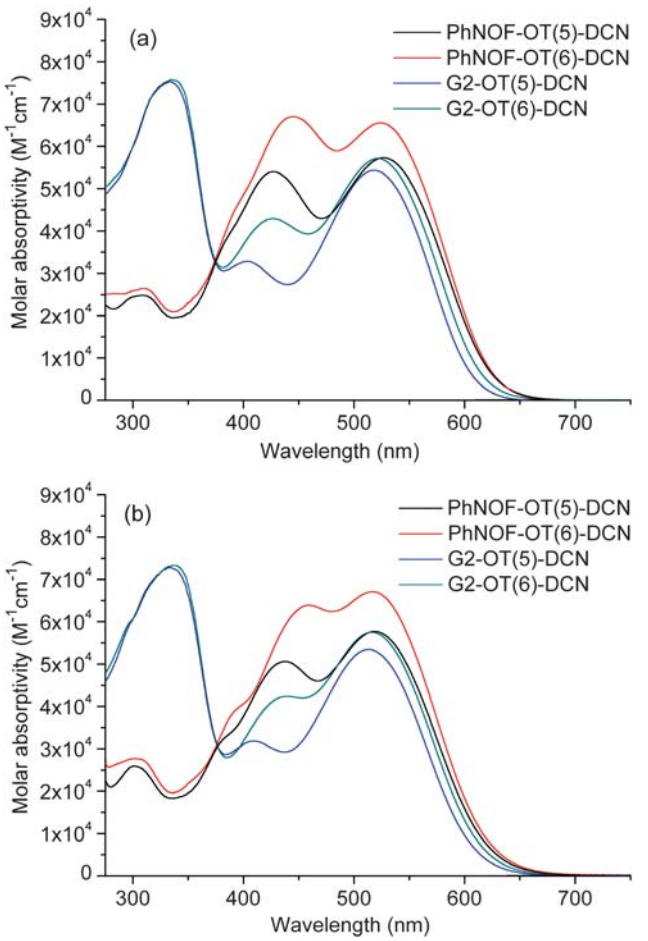


**Fig. 2** Absorption spectra of **PhNOF-OT(*n*)-DCN** and **$G_2$-OT(*n*)-DCN** in (a) chloroform and (b) DMSO.

polarity of solvent. There is no observable fluorescence emission upon irradiating at $\lambda_{max}^{abs}$ which is attributed to the strong charge-transfer character of these donor–acceptor oligothiophenes. These oligomers showed pronounced peak broadening and red shifts of ~40 nm of absorption cutoff upon formation into thin films which is attributed to the planarization of aryl rings and the presence of interchain interactions in the solid state, resulting in the optical band gap reducing to 1.85 eV.

Both **PhNOF-OT(*n*)-DCN**s and **$G_2$-OT(*n*)-DCN**s exhibit very similar electrochemical redox behavior. All the oligothiophenes showed three oxidation waves with $E_{oxd1}$ at 0.30–0.35 V, $E_{oxd2}$ at 0.39–0.48 V, and $E_{oxd3}$ at 0.73–0.86 V ($E_{1/2}$ ($Fc/Fc^+$) = 0.49 V *vs.* SCE) corresponding to the sequential removal of electrons from the arylamino group(s), the oligothiophene core or the interior carbazole moieties, and the oligothiophene core, respectively. (Fig. 3) They also exhibit two reduction waves ($E_{red1} = -1.50$ V and $E_{red2} = -2.00$ V *vs.* $Fc/Fc^+$) corresponding to the reductions of dicyanovinyl group and the reduction of oligothiophene core, respectively. Hence, the HOMO and LUMO levels of these oligothiophenes were estimated to be ~−5.2 eV and ~−3.3 eV, respectively based on CV data.

The potential of these highly extended oligothiophenes as hole-transporting light-absorbing materials in solution-processable photovoltaic cells was explored. The bulk heterojunction PV cells with a device structure of ITO/PEDOT : PSS/oligomer : PCBM/LiF (1 nm)/Al (120 nm) were fabricated by the spin-casting of a PEDOT-PSS layer and then a blend of oligomer : PCBM layer followed by vacuum deposition of LiF and Al as the cathode. The PV responses of these devices were measured under AM 1.5 simulated solar illumination at an irradiation intensity of 100 mW $cm^{-2}$. The results of the device performance are summarized in Table 2. Most of the devices have relatively large $V_{oc}$ (~ 0.8 V) because of the low-lying HOMO levels of these oligothiophenes (~ −5.2 eV) resulting in larger differences to the LUMO level of PCBM. The devices with a thicker active layer have better PCEs and fill factors. By increasing the film thickness from 100 nm to 160 nm, devices fabricated with 1 : 2 **$G_2$-OT(6)-DCN**:PCBM ratios exhibit a significant increase in $J_{sc}$ and *PCE* up to 1.12% with $V_{oc}$ of 0.79 V (Fig. 4). It is known that the carrier mobility of a blended film is greatly influenced by the donor : acceptor ratio. **$G_2$-OT(6)-DCN**:PCBM-based devices with a ratio of 1 : 4 exhibit decreases in $J_{sc}$, $V_{oc}$ and thus, *PCE*. In sharp contrast, devices fabricated with 1 : 4 **PhNOF-OT(5)-DCN**:PCBM ratios exhibit dramatic enhancement in $J_{sc}$ (to 5.41 mA $cm^{-2}$) and *FF* (= 0.40) with a *PCE* up to 1.72% (Fig. 5). The external quantum efficiency (EQE) measurements show that the **PhNOF-OT(5)-DCN**-based device exhibits a very broad

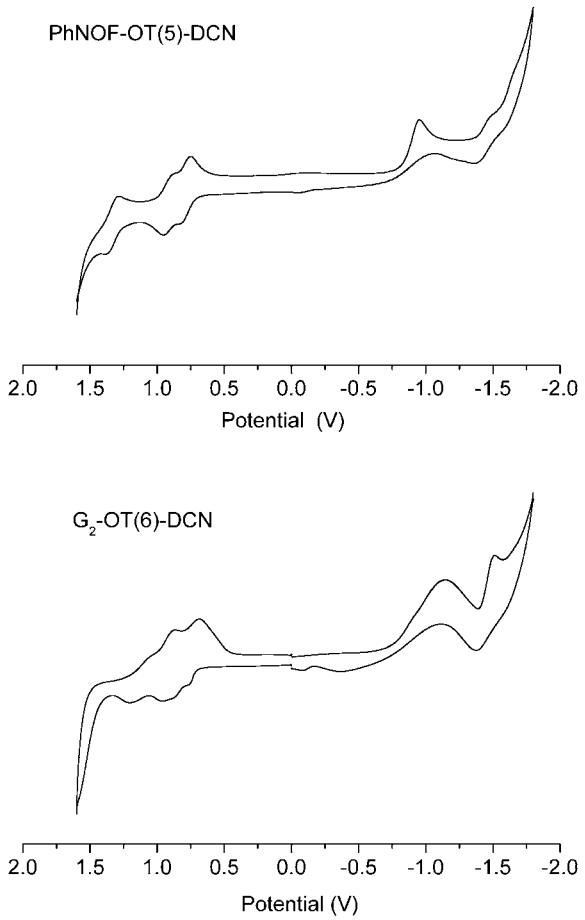


**Fig. 3** CV traces of **PhNOF-OT(5)-DCN** and **$G_2$-OT(6)-DCN**.

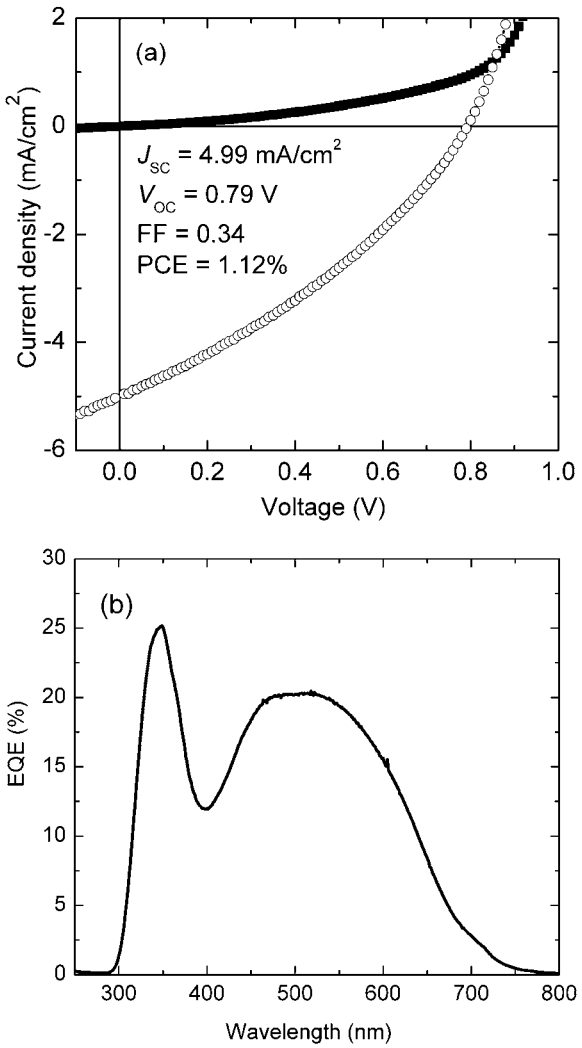


**Fig. 4** (a) *J–V* characteristics of **$G_2$-OT(6)-DCN** : PCBM (1 : 2)-based PV cells (b) the EQE curves of the corresponding PV cells.

photoresponse range from 300 nm to 680 nm which corresponds well to the UV-vis absorption spectra of the films and the maximum EQE reaches 43% at 424 nm. Our findings highlight the potential of this class of materials for further device optimization in high performance PV applications.

## Conclusions

In summary, a novel series of solution-processable, p-type, low-optical-gap semiconductors based on penta- and hexa-thiophenes asymmetrically endcapped with a triarylamine or triarylamino-substituted dendron and dicyanovinyl groups has been synthesized. A highly extended oligothiophene backbone results in strong spectra broadening which is advantageous

**Table 2** Summary of PV device performance with a device structure of ITO/PEDOT : PSS/oligomer : PCBM/LiF (0.95 nm)/Al (130 nm)

| Active layer | Thin thickness/nm | $J_{SC}$/mA cm$^{-2}$ | $V_{OC}$/V | *FF* | *PCE* (%)[a,b] | $EQE_{max}$ (%) |
|---|---|---|---|---|---|---|
| **PhNOF-OT(5)-DCN** : PCBM | 85 | 2.94 | 0.93 | 0.17 | 0.47 | 37 |
| (1 : 2) | 160 | 4.97 | 0.83 | 0.28 | 0.97 | 47 |
| **PhNOF-OT(5)-DCN** : PCBM | 106 | 4.16 | 0.79 | 0.31 | 1.03 | 40 |
| (1 : 4) | 147 | 5.41 | 0.79 | 0.40 | 1.72 | 43 |
| **PhNOF-OT(6)-DCN** : PCBM | 81 | 1.78 | 0.79 | 0.52 | 0.73 | 18 |
| (1 : 2) | 102 | 1.96 | 0.75 | 0.52 | 0.76 | 17 |
| **$G_2$-OT(5)-DCN** : PCBM (1 : 2) | 110 | 4.30 | 0.54 | 0.32 | 0.63 | 11 |
| **$G_2$-OT(6)-DCN** : PCBM (1 : 2) | 100 | 3.90 | 0.81 | 0.35 | 1.11 | 28 |
| | 160 | 4.99 | 0.79 | 0.34 | 1.12 | 25 |
| **$G_2$-OT(6)-DCN** : PCBM (1 : 4) | 103 | 3.26 | 0.52 | 0.33 | 0.56 | 27 |
| | 141 | 3.68 | 0.66 | 0.35 | 0.84 | 26 |

[a] $J_{sc}$ and *PCE* have been calibrated using external quantum efficiency measurement. [b] Under simulated AM 1.5 solar irradiation of 100 mW cm$^{-2}$ for as-fabricated devices.

 

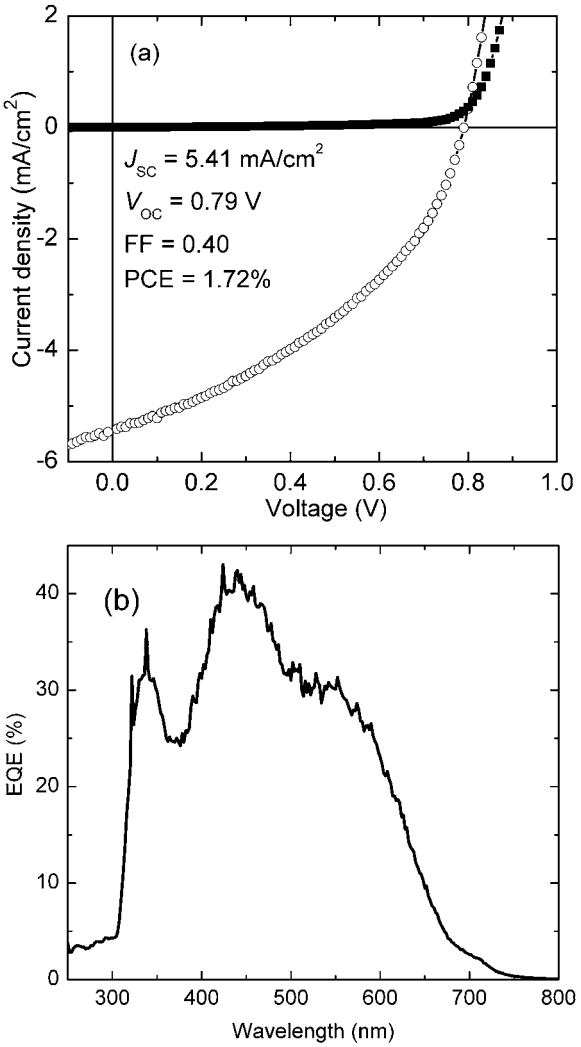


**Fig. 5** (a) *J–V* characteristics of **PhNOF-OT(5)-DCN** : PCBM (1 : 4)-based PV cells (b) the EQE curves of the corresponding PV cells.

to light harvesting. The **PhNOF-OT(5)-DCN** : PCBM-based device exhibits a high *PCE* of 1.72% with $V_{oc}$ = 0.79 V and $EQE_{max}$ = 43%. Our findings also suggest that highly extended donor–acceptor oligomers can be useful as a p-type, low bandgap semiconductor for solution-processable bulk heterojunction PV cells. Further device optimization to enhance the efficiency of these oligomer-based PV cells is still in progress.

## Experimental

### General procedures and requirements

All the solvents were dried by the standard methods wherever needed. $^1$H NMR spectra were recorded using a Bruker-400 NMR spectrometer and referenced to the residual $CHCl_3$ 7.26 ppm. $^{13}$C NMR spectra were recorded using a Bruker-400 NMR spectrometer and referenced to the $CDCl_3$ 77 ppm. Mass spectroscopy (MS) measurements were carried using fast atom bombardment on the API ASTER Pulser I Hybrid Mass Spectrometer or matrix-assisted laser desorption ionization-time-of-flight (MALDI-TOF) technique. Elemental Analysis was carried out on a CARLO ERBA 1106 Elemental Analyzer. Thermal stabilities were determined using a thermal gravimetric analyzer (PE-TGA6) with a heating rate of 10 °C min$^{-1}$ under $N_2$. The glass transition and melting transition were extracted from the second run DSC traces which were determined by differential scanning calorimeter (PE PYRIS Diamond DSC) with a heating rate of 10 °C min$^{-1}$ under $N_2$. All absorption measurements were performed with a Varian Cary 100-UV-Vis spectrophotometer. The half-wave potential ($E_{1/2}$) or peak potential ($E_p$) *vs.* $F_C^+/F_C$ were estimated by a cyclic voltammetric method (Voltammetric Analyzer CV-50W) using a platinum disc electrode as the working electrode, a platinum wire as the counter electrode, and SCE as the reference electrode with an agar bridge connecting to the oligomer solution dissolved in $CH_2Cl_2$ using 0.1 M of $Bu_4NPF_6$ as the supporting electrolyte with a scan rate of 100 mV s$^{-1}$ and all the potentials were calibrated with ferrocene as an external standard.

### OPV device fabrication and testing

ITO-coated glass substrates (15 Ω/□) were patterned by a conventional wet-etching process using an acid mixture of HCl (6 N) and $HNO_3$ (0.6 N) as the etchant. The active area of each solar cell was 5 × 7 mm$^2$. After patterning, the substrates were rinsed in deionized water, and then ultrasonicated sequentially in acetone (20 °C) and 2-propanol (65 °C). Immediately before device fabrication, the ITO substrate was treated in a UV-ozone oven for 15 min. Subsequently, a poly(3,4-ethylenedioxythiophene)-poly(styrene sulfonate) (PEDOT-PSS) thin film (50 nm) was spin-coated at 5000 rpm from its aqueous solution onto the treated substrate, and then baked at 140 °C under nitrogen for 30 min. The active layer composed of the blend of oligomer and PCBM at various ratios was then spin-coated on top of PEDOT-PSS from chlorobenzene solutions for 60 s. The thickness of the resulting film was measured with a Dektak III surface profilometer. The device fabrication was completed by the vacuum deposition of LiF (1 nm) and Al cathode (120 nm). The solar cells with no protective encapsulation were subsequently tested in air under air mass (AM) 1.5 simulated solar illumination (100 mW cm$^{-2}$, Sciencetech, Model SF150). Current–voltage (*I–V*) characteristics were recorded using a computer-controlled Keithley 2400 source meter.

**2-[9,9-Bis(*n*-decyl)-2-diphenylamino-7-fluorenyl]-bithiophene (3).** To a 100 mL round bottom flask was added 1.4 g (2.13 mmol) of boronic acid **1**, 5-iodo-2,2′-bithiophene **2** (746 mg, 2.56 mmol), 100 mg of $Pd(PPh_3)_4$, 5 mL of 2 M $K_2CO_3$ and 40 mL of THF. The mixture was heated to 80 °C and stirred overnight under $N_2$. After cooling to room temperature, the mixture was poured into water and extracted with DCM (3 × 20 mL). The combined organic phase was dried over anhydrous sodium sulfate, filtered and evaporated under reduced pressure. The crude product was purified by silica gel column chromatography using PE–DCM as eluent affording the desired product as a colorless crystalline solid (1.2 g, 73%). Mp: 72–74 °C. $^1$H NMR (400 MHz, $CDCl_3$): $\delta$ 7.54–7.60 (m, 3 H), 7.49 (d, $J$ = 0.8 Hz, 1 H), 7.20–7.27 (m, 6 H), 7.17 (d, $J$ = 4.0 Hz, 1 H), 7.10–7.12 (m, 5 H), 6.99–7.04 (m, 4 H), 1.80–1.95 (m, 4 H), 1.05–1.27 (m, 28 H), 0.86 (t, $J$ = 2.8 Hz, 6 H), 0.67–0.69 (m, 4 H). $^{13}$C NMR

(100 MHz, $CDCl_3$): $\delta$ 152.3, 151.4, 147.9, 147.2, 144.0, 140.6, 137.6, 136.1, 135.7, 132.0, 129.1, 127.8, 124.6, 124.5, 124.2, 123.8, 123.5, 123.4, 123.2, 122.5, 120.4, 119.6, 119.4, 119.2, 55.1, 40.2, 31.9, 29.9, 29.7, 29.6, 29.5, 29.3, 23.8, 22.6, 14.1. MS (MALDI-TOF): *m*/*z* 778.1 ($M^+$ + 1).

**5-[9,9-Bis(*n*-decyl)-2-diphenylamino-7-fluorenyl]-2-pentathiophenecarboxaldehyde (6a).** To a dry 100 mL two-neck flask containing 2.0 g (2.57 mmol) of **3** and 30 mL of dry THF was dropwise added 2.4 mL (3.9 mmol) of 1.6 M of *n*-butyl lithium under $N_2$ at −78 °C while maintaining a good stirring. After stirring for 1 h, trimethyl borate (0.45 mL, 4.0 mmol) was added in one portion. The reaction mixture was then stirred for 1 h at −78 °C. When the mixture was naturally warmed to −30 °C, water and HCl (3 M) were added. Then the solution mixture was poured into water and extracted with EA (3 × 50 mL). The combined organic phase was dried over anhydrous sodium sulfate, filtered and evaporated to dryness at 35 °C. The crude product was purified by silica gel column chromatography using DCM and PE–EA as eluent affording the desired product, 5-[9,9-bis(*n*-decyl)-2-diphenylamino-7-fluorenyl]-2-bithiopheneboronic acid (**4**) as a green solid (1.58 g, 75%). The product was directly used in the next coupling reaction without further purification. To a 100 mL round bottom flask was added 300 mg (0.36 mmol) of boronic acid **4**, 100 mg (0.25 mmol) of aldehyde (**5a**), 50 mg of $Pd(PPh_3)_4$, 2 mL of 2 M $K_2CO_3$ and 20 mL of THF. The mixture was heated to 80 °C and stirred overnight under $N_2$. After cooling to room temperature, the mixture was poured into water and extracted with DCM (3 × 20 mL). The combined organic phase was dried with anhydrous sodium sulfate, filtered and evaporated to dryness. The crude product was purified by silica gel column chromatography using PE–DCM as eluent affording the desired product as a red solid (205 mg, 78%). Mp: 145–147 °C. $^1$H NMR (400 MHz, $CDCl_3$): $\delta$ 9.86 (s, 1 H), 7.67 (d, $J$ = 4.0 Hz, 1 H), 7.54–7.60 (m, 3 H), 7.49 (d, $J$ = 1.2 Hz, 1 H), 7.23–7.28 (m, 7 H), 7.17 (d, $J$ = 4.0 Hz, 1 H), 7.09–7.14 (m, 10 H), 6.99–7.03 (m, 3 H), 1.81–1.96 (m, 4 H), 1.07–1.25 (m, 28 H), 0.86 (t, $J$ = 2.8 Hz, 6 H), 0.67–0.70 (m, 4 H). $^{13}$C NMR (100 MHz, $CDCl_3$): $\delta$ 182.4, 152.3, 151.5, 147.9, 147.3, 146.7, 144.5, 141.6, 140.8, 138.8, 137.4, 137.0, 136.9, 135.6, 135.5, 135.2, 135.1, 134.5, 131.8, 129.2, 127.0, 125.2, 124.8, 124.7, 124.6, 124.3, 124.1, 124.0, 123.9, 123.5, 123.4, 122.6, 120.4, 119.6, 119.5, 119.2, 55.1, 40.2, 31.9, 29.9, 29.6, 29.5, 29.3, 23.8, 22.7, 14.1. MS (MALDI-TOF): *m*/*z* 1052.2 ($M^+$ + 1).

**5-[9,9-Bis(*n*-decyl)-2-diphenylamino-7-fluorenyl]-2-hexathiophenecarboxaldehyde (6b).** The synthetic procedure for compound **6a** was followed using 300 mg (0.36 mmol) of boronic acid **4**, 121 mg (0.25 mmol) of aldehyde **5b**, 50 mg of $Pd(PPh_3)_4$, 2 mL of 2 M $K_2CO_3$ and 20 mL of 1,4-dioxane. The crude product was purified by silica gel column chromatography using PE–DCM as eluent affording the desired product as a red solid (227 mg, 80%). Mp: 162–164 °C. $^1$H NMR (400 MHz, $CDCl_3$): $\delta$ 9.86 (s, 1 H), 7.68 (d, $J$ = 3.6 Hz, 1 H), 7.54–7.60 (m, 3 H), 7.49 (d, $J$ = 1.2 Hz, 1 H), 7.23–7.29 (m, 7 H), 7.18 (d, $J$ = 4.0 Hz, 1 H), 7.10–7.15 (m, 12 H), 6.99–7.03 (m, 3 H), 1.81–1.96 (m, 4 H), 1.07–1.25 (m, 28 H), 0.86 (t, $J$ = 2.8 Hz, 6 H), 0.67–0.70 (m, 4 H). $^{13}$C NMR (100 MHz, $CDCl_3$): $\delta$ 182.4, 152.3, 151.5, 147.9, 147.3, 146.7, 144.4, 141.6, 140.8, 138.7, 137.4, 137.0, 136.9, 136.7, 136.5, 135.6, 135.5, 135.2, 134.6, 131.9, 129.2, 127.0, 125.2, 124.8, 124.7, 124.6, 124.5, 124.4, 124.3, 124.1, 123.9, 123.4, 122.5, 120.4, 119.6, 119.5, 119.2, 55.1, 40.2, 31.9, 29.9, 29.6, 29.5, 29.3, 23.8, 22.6,14.1. MS (MALDI-TOF): *m*/*z* 1134.3 ($M^+$ + 1).

**PhNOF-OT(5)-DCN.** To a 100 mL round bottom flask containing 210 mg (0.20 mmol) of **6a** and 10 mL of $CHCl_3$ was added 0.40 g (6.1 mmol) of malononitrile and 0.8 mL of pyridine at room temperature. The solution was heated to reflux and stirred overnight under $N_2$. After cooling to room temperature, the reaction mixture was poured into water, neutralized with 0.1 M HCl, and extracted with $CHCl_3$ (3 × 20 mL). The combined organic phase was washed with water, dried over anhydrous sodium sulfate, filtered and evaporated to dryness. The crude product was purified by silica gel column chromatography using PE–DCM as eluent and further precipitated by $CHCl_3$–$Et_2O$, washed with methanol and dried under vacuum affording the desired product as a black red solid (204 mg, 93%). $^1$H NMR (400 MHz, $CDCl_3$): $\delta$ 7.73 (s, 1 H), 7.54–7.62 (m, 4 H), 7.49 (d, $J$ = 1.2 Hz, 1 H), 7.35 (d, $J$ = 4.0 Hz, 1 H), 7.23–7.29 (m, 6 H), 7.09–7.18 (m, 11 H), 6.99–7.03 (m, 3 H), 1.83–1.94 (m, 4 H), 1.07–1.27 (m, 28 H), 0.86 (t, $J$ = 7.2 Hz, 6 H), 0.67–0.70 (m, 4 H); $^{13}$C NMR (100 MHz, $CDCl_3$): $\delta$ 152.3, 151.5, 149.8, 148.8, 147.9, 147.3, 144.5, 140.9, 140.2, 140.1, 137.5, 137.1, 135.5, 135.4, 135.0, 134.6, 133.5, 133.3, 131.8, 129.2, 128.1, 125.6, 124.8, 124.7, 124.6, 124.3, 124.2, 124.1, 123.9, 123.4, 122.6, 120.4, 119.6, 119.5, 119.1, 114.2, 113.5, 75.9, 55.1, 40.2, 31.9, 29.9, 29.6, 29.5, 29.3, 23.9, 22.6, 14.1. HRMS (MALDI-TOF): calcd: For $C_{69}H_{69}N_3S_5$: 1099.4089; Found: 1089.4092. Anal calc. for $C_{69}H_{69}N_3S_5$: C 75.30, H 6.32, N 3.82; found: C 75.36, H 6.33, N 3.84.

**PhNOF-OT(6)-DCN.** The synthetic procedure for **PhNOF-OT(5)-DCN** was followed using 226 mg (0.20 mmol) of **6b**, 0.40 g (6.1 mmol) of malononitrile, 0.8 mL of pyridine and 10 mL of $CHCl_3$. The crude product was purified by silica gel column chromatography using PE–DCM and precipitated by $CHCl_3$–$Et_2O$ affording the desired product as a black red solid (212 mg, 90%). $^1$H NMR (400 MHz, $CDCl_3$): $\delta$ 7.74 (s, 1 H), 7.55–7.63 (m, 4 H), 7.49 (s, 1 H), 7.35 (d, $J$ = 4.0 Hz, 1 H), 7.23–7.29 (m, 6 H), 7.09–7.18 (m, 13 H), 6.99–7.03 (m, 3 H), 1.81–1.95 (m, 4 H), 1.07–1.25 (m, 28 H), 0.86 (t, $J$ = 6.8 Hz, 6 H), 0.67–0.70 (m, 4 H). $^{13}$C NMR (100 MHz, $CDCl_3$): $\delta$ 153.3, 151.5, 149.8, 148.8, 147.9, 147.3, 144.4, 140.8, 140.1, 137.4, 136.8, 136.6, 135.6, 135.5, 135.3, 134.7, 133.5, 133.4, 131.8, 129.2, 128.2, 125.6, 124.9, 124.8, 124.7, 124.6, 124.4, 124.3, 124.1, 123.9, 123.4, 122.6, 120.5, 119.6, 119.5, 119.2, 114.2, 113.5, 75.9, 55.1, 40.2, 31.9, 30.9, 29.9, 29.6, 29.5, 29.3, 23.9, 22.7, 14.1. HRMS (MALDI-TOF): calcd: For $C_{73}H_{71}N_3S_6$: 1181.3966; Found: 1181.4034. Anal calc. for $C_{73}H_{71}N_3S_6$: C 74.13, H 6.05, N 3.55; found: C 74.42, H 6.07, N 3.71.

**5-{3,6-Bis[4-(diphenylamino)-1-phenyl]carbazol-9-yl}-2-pentathiophene-carboxaldehyde (8a).** The synthetic procedure for compound **6a** was followed using 430 mg (0.5 mmol) of boronic acid **7**, 161 mg (0.4 mmol) of aldehyde **5a**, 40 mg of $Pd(PPh_3)_4$, 3 mL of 2 M $K_2CO_3$ and 20 mL of THF. The crude product was purified by silica gel column chromatography using PE–DCM as eluent affording the desired product as a red solid (362 mg, 83%). Mp: 298–300 °C.$^1$H NMR (400 MHz, $CDCl_3$): $\delta$ 9.86 (s, 1 H),

 

9.88 (s, 1 H), 8.32 (d, $J = 1.2$ Hz, 2 H), 7.67–7.70 (m, 3 H), 7.61 (d, $J = 8.4$ Hz, 6 H), 7.24–7.29 (m, 11 H), 7.13–7.16 (m, 18 H), 7.02–7.05 (m, 4 H). $^{13}$C NMR (100 MHz, $CDCl_3$): $\delta$ 182.4, 147.7, 146.7, 146.6, 141.7, 141.3, 138.6, 137.5, 137.4, 136.7, 136.2, 136.0, 135.8, 135.4, 135.1, 134.7, 134.1, 129.3, 127.9, 126.9, 125.6, 125.3, 125.2, 124.7, 124.67, 124.61, 124.3, 124.2, 124.1, 122.8, 122.5, 118.3, 110.6. MS (MALDI-TOF): $m/z$ 1092.1 ($M^+ + 1$).

**5-{3,6-Bis[4-(diphenylamino)-1-phenyl]carbazol-9-yl}-2-hexathiophene-carboxaldehyde (8b).** The synthetic procedure for compound **6b** was followed using 430 mg (0.5 mmol) of boronic acid **7**, 145 mg (0.30 mmol) of aldehyde **5b**, 3 mL of 2 M $K_2CO_3$ and 20 mL of 1,4-dioxane. The crude product was purified by silica gel column chromatography using PE–DCM as eluent affording the desired product as a red solid (281 mg, 80%). Mp: 302–305 °C. $^1$H NMR (400 MHz, $CDCl_3$): $\delta$ 9.87 (s, 1 H), 8.32 (d, $J = 1.6$ Hz, 2 H), 7.68–7.71 (m, 3 H), 7.61 (d, $J = 8.4$ Hz, 6 H), 7.24–7.30 (m, 11 H), 7.13–7.21 (m, 20 H), 7.02–7.05 (m, 4 H). $^{13}$C NMR (100 MHz, $CDCl_3$): $\delta$ 182.4, 147.7, 146.7, 146.6, 141.6, 141.3, 138.7, 137.4, 137.3, 136.8, 136.2, 136.0, 135.8, 135.3, 135.2, 134.6, 134.0, 129.3, 127.9, 127.0, 125.6, 125.4, 125.2, 124.7, 124.6, 124.57, 124.52, 124.3, 124.2, 124.1, 122.8, 122.4, 118.3, 110.6. MS (MALDI-TOF): $m/z$ 1174.3 ($M^+ + 1$).

**$G_2$-OT(5)-DCN.** The synthetic procedure for compound **PhNOF-OT(5)-DCN** was followed using 160 mg (0.146 mmol) of **8a**, 400 mg (6.1 mmol) of malononitrile, 0.7 mL of pyridine and 10 mL of $CHCl_3$. The crude product was purified by silica gel column chromatography using PE–DCM and precipitated by $CHCl_3$–$Et_2O$ affording the desired product as a black solid (149 mg, 89%). $^1$H NMR (400 MHz, $CDCl_3$): $\delta$ 8.32 (d, $J = 1.2$ Hz, 2 H), 7.72 (s, 1 H), 7.69 (dd, $J = 8.8$ Hz, $J = 1.6$ Hz 2 H), 7.61 (d, $J = 8.4$ Hz, 7 H), 7.35 (d, $J = 4.0$ Hz, 1 H), 7.23–7.29 (m, 10 H), 7.12–7.20 (m, 18 H), 7.05 (t, $J = 7.4$ Hz, 4 H). $^{13}$C NMR (100 MHz, $CDCl_3$): $\delta$ 149.9, 148.8, 147.8, 146.8, 141.3, 140.1, 140.0, 137.6, 137.3, 136.4, 135.9, 135.8, 135.1, 135.0, 134.1, 133.7, 133.5, 129.3, 128.2, 127.9, 125.7, 125.4, 125.0, 124.9, 124.8, 124.7, 124.4, 124.3, 124.2, 122.8, 122.6, 118.4, 114.3, 113.5, 110.6, 76.1. HRMS (MALDI-TOF): calcd: For $C_{72}H_{45}N_5S_5$: 1139.2273; Found: 1139.2288. Anal calc. for $C_{72}H_{45}N_5S_5$: C 75.82, H 3.98, N 6.14; found: C 75.87, H 3.99, N 6.03.

**$G_2$-OT(6)-DCN.** The synthetic procedure for compound **PhNOF-OT(5)-DCN** was followed using 170 mg (0.144 mmol) of **8b**, 400 mg (6.1 mmol) of malononitrile, 0.7 mL of pyridine and 10 mL of $CHCl_3$. The crude product was purified by silica gel column chromatography using PE–DCM and precipitated by $CHCl_3$–$Et_2O$ affording the desired product as a black solid (161 mg, 91%). $^1$H NMR (400 MHz, $CDCl_3$): $\delta$ 8.32 (d, $J = 1.2$ Hz, 2 H), 7.74 (s, 1 H), 7.70 (dd, $J = 8.8$ Hz, $J = 1.6$ Hz, 2 H), 7.59–7.62 (m, 7 H), 7.36 (d, $J = 4.0$ Hz, 1 H), 7.25–7.30 (m, 10 H), 7.12–7.21 (m, 20 H), 7.02–7.06 (m, 4 H). $^{13}$C NMR (100 MHz, $CDCl_3$): $\delta$ 149.8, 148.7, 147.7, 146.7, 141.2, 140.1, 140.0, 137.4, 137.3, 136.4, 136.0, 135.7, 135.6, 135.0, 134.9, 134.0, 133.6, 133.4, 129.3, 128.1, 127.9, 125.6, 125.2, 124.8, 124.7, 124.5, 124.3, 122.8, 122.4, 118.3, 114.2, 113.5, 110.6, 75.8. HRMS (MALDI-TOF): calcd: For $C_{76}H_{47}N_5S_6$: 1221.2150; Found: 1221.2121. Anal calc. for $C_{76}H_{47}N_5S_6$: C 74.66, H 3.87, N 5.73; found: C 74.77, H 3.99, N 5.58.

## Acknowledgements

This work was financially supported by Hong Kong Research Grant Council, GRF, HKBU 202408.

## References

1 H. Hoppe and N. S. Sariciftci, *J. Mater. Chem.*, 2006, **16**, 45; S. Günes, H. Neugebauer and N. S. Sariciftci, *Chem. Rev.*, 2007, **107**, 1324; B. C. Thompson and J. M. Fréchet, *Angew. Chem., Int. Ed.*, 2008, **47**, 58.
2 F. C. Krebs, *Sol. Energy Mater. Sol. Cells*, 2009, **93**, 394; F. C. Krebs, S. A. Gevorgyan and J. Alstrup, *J. Mater. Chem.*, 2009, **19**, 5442; F. C. Krebs, *Sol. Energy Mater. Sol. Cells*, 2009, **93**, 465; F. C. Krebs, M. Jørgensen, K. Norrman, O. Hagemann, J. Alstrup, T. D. Nielsen, J. Fyenbo, K. Larsen and J. Kristensen, *Sol. Energy Mater. Sol. Cells*, 2009, **93**, 422.
3 G. Li, V. Shrotriya, J. Huang, Y. Yao, T. Moriarty, K. Emery and Y. Yang, *Nat. Mater.*, 2005, **4**, 826; Y. Kim, S. Cook, S. M. Tuladhar, S. A. Choulis, J. Nelson, J. R. Durrant, D. D. C. Bradley, M. Giles, I. Mcculloch, C. S. Ha and M. Ree, *Nat. Mater.*, 2006, **5**, 197; J. Hou, H.-Y. Chen, S. Zhang, G. Li and Y. Yang, *J. Am. Chem. Soc.*, 2008, **130**, 16144; Y. Liang, D. Feng, Y. Wu, S. Tsai, G. Li, C. Ray and L. Yu, *J. Am. Chem. Soc.*, 2009, **131**, 7792; Y. Liang, Y. Wu, D. Feng, S. Tsai, H. Son, G. Li and L. Yu, *J. Am. Chem. Soc.*, 2009, **131**, 56; S. H. Park, A. Roy, S. Beaupre, S. Cho, N. Coates, J. S. Moon, D. Moses, M. Leclerc, K. Lee and A. J. Heeger, *Nat. Photonics*, 2009, **3**, 297.
4 M. Jørgensen, K. Norrman and F. C. Krebs, *Sol. Energy Mater. Sol. Cells*, 2008, **92**, 686.
5 J. Lu, P. F. Xia, P. K. Lo, Y. Tao and M. S. Wong, *Chem. Mater.*, 2006, **18**, 6194; S. Roquet, A. Cravino, P. Leriche, O. Alévêque, P. Frère and J. Roncali, *J. Am. Chem. Soc.*, 2006, **128**, 3459; A. Cravino, S. Roquet, P. Leriche, O. Alévêque, P. Frère and J. Roncali, *Chem. Commun.*, 2006, 1416; K. Schulze, C. Uhrich, R. Schüppel, K. Leo, M. Pfeiffer, E. Brier, E. Reinold and P. Bäuerle, *Adv. Mater.*, 2006, **18**, 2872; F. Silvestri, M. D. Irwin, L. Beverina, A. Facchetti, G. A. Pagani and T. J. Marks, *J. Am. Chem. Soc.*, 2008, **130**, 17640; P. F. Xia, J. P. Lu, C. H. Kwok, H. Fukutani, M. S. Wong and Y. Tao, *J. Polym. Sci., Part A: Polym. Chem.*, 2009, **47**, 137; M. Velusamy, J.-H. Huang, Y.-C. Hsu, H.-H. Chou, K.-C. Ho, P. L. Wu, W.-H. Chang, J. T. Lin and C.-W. Chu, *Org. Lett.*, 2009, **11**, 4898.
6 A. Marrocchi, F. Silvestri, M. Seri, A. Facchetti, G. A. Taticchi and T. J. Marks, *Chem. Commun.*, 2009, 1380.
7 J. A. Mikroyannidis, M. M. Stylianakis, P. Suresh, P. Balraju and G. D. Sharma, *Org. Electron.*, 2009, **10**, 1320.
8 A. B. Tamayo, X.-D. Dang, B. Walker, J. Seo, T. Kent and T.-C. Nguyen, *Appl. Phys. Lett.*, 2009, **94**, 103301.
9 C. Soci, I. W. Hwang, D. Moses, Z. Zhu, D. Waller, R. Guadiana, C. J. Brabec and A. J. Heeger, *Adv. Funct. Mater.*, 2007, **17**, 632.
10 P. F. Xia, X. J. Feng, J. P. Lu, R. Movileanu, Y. Tao, J. M. Baribeau and M. S. Wong, *J. Phys. Chem. C*, 2008, **112**, 16714; P. F. Xia, X. J. Feng, J. P. Lu, S. W. Tsang, R. Movileanu, Y. Tao and M. S. Wong, *Adv. Mater.*, 2008, **20**, 4810.